A study of mass transfer in the membrane air-stripping process using microporous polyproplylene hollow fibers

Mahmud, Hassan; Kumar, Ashwani; Narbaitz, Robert M.; Matsuura, Takeshi

Publisher's version / Version de l'éditeur:
https://doi.org/10.1016/S0376-7388(00)00381-1
Journal of Membrane Science, 179, 1-2, pp. 29-41, 2000-11-15

ELSEVIER

Journal of Membrane Science 179 (2000) 29–41

journal of MEMBRANE SCIENCE

www.elsevier.nl/locate/memsci

A study of mass transfer in the membrane air-stripping process using microporous polyproplylene hollow fibers

Hassan Mahmud [a], Ashwani Kumar [b,*], Roberto M. Narbaitz [c], Takeshi Matsuura [a]

[a] *Industrial Membrane Research Institute, Department of Chemical Engineering, University of Ottawa, Ottawa, Ont., Canada K1N 6N5*

[b] *Institute of Chemical Process and Environmental Technology, National Research Council Canada, Montreal Road, Ottawa, Ont., Canada K1A 0R6*

[c] *Department of Civil Engineering, University of Ottawa, Ottawa, Ont., Canada K1N 6N5*

Received 22 October 1999; received in revised form 3 March 2000; accepted 6 March 2000

Abstract

The mass transfer of water and chloroform in membrane air-stripping (MAS) was studied using a microporous polypropylene hollow fiber membrane module, with air flow on the lumen side and liquid cross-flow on the shell side. Water transport experiments showed that its mass transport decreased significantly when the membrane had been in contact with water for prolonged periods. It was hypothesized that the increased mass transfer resistance was due to water condensation in a fraction of the membrane pores. MAS of chloroform from aqueous solutions confirmed the additional mass transfer resistance with prior exposure to water. It was concluded that membrane pores were either completely air-filled or partially wetted with water during the MAS process. Existing models are able to predict the performance only for either completely air-filled or liquid-filled pores. A modified model was proposed to take into account the diffusion through partially wetted pores. The model described the data well. This hypothesis also provided a plausible explanation to the conflicting literature values of the membrane mass transfer resistance. It was found that the membrane mass transfer resistance of the partially wetted pores is two orders of magnitude higher than that of air-filled pores. The overall mass transfer coefficient was constant for initial feed chloroform concentrations ranging from 50 to 1000 ppm.

Keywords: Mass transfer resistance; Membrane air-stripping; Microporous membranes; Organic separation; Water treatment

1. Introduction

Membrane air-stripping (MAS), using microporous polypropylene hollow fiber membrane modules, is one of the processes with a great potential for the removal and recovery of volatile organic compounds (VOCs) from water/wastewater [1]. Mass transfer resistances in MAS processes have been studied by many researchers [2–10]. The overall liquid phase based mass transfer coefficient (K_L) for MAS is usually lower than that for the conventional air-stripping process due to the mass transfer resistance ($1/(k_m H)$) created by the membrane itself [2,4]. There are controversial views regarding the importance of membrane mass transfer resistance for air-filled pores [3,4,7,9]. Semmens et al. [3] in their work on MAS of VOCs from aqueous solutions without chemical reaction predicted individual local liquid phase, local gas phase and membrane mass transfer resistances

* Corresponding author. Fax: +1-613-941-2529.
E-mail address: ashwani.kumar@nrc.ca (A. Kumar).

0376-7388/00/$ – see front matter
PII: S0376-7388(00)00381-1

Nomenclature

a	surface to volume ratio, m^2/m^3
C_0	VOC concentration in the reservoir at time 0, ppm
C_t	VOC concentration in the reservoir at time t, ppm
d_i	inner diameter of the hollow fiber, m
d_o	outer diameter of the hollow fiber, m
D_{Kn}	Knudsen diffusion coefficient in air, m^2/s
D_c^{ch}	continuum diffusion coefficient of chloroform in air phase, m^2/s
D_{eff}^{ch}	effective diffusion coefficient of chloroform in air, m^2/s
D_w^{ch}	diffusion coefficient of chloroform in water, m^2/s
D_c^w	continuum diffusion coefficient of water in air phase, m^2/s
D_{eff}^w	effective diffusion coefficient of water in air, m^2/s
h	length of the hollow fiber module compartment ($0.5L$), m
H	dimensionless Henry's Law constant
k	slope
k_a	local air phase mass transfer coefficient, m/s
k_L	local liquid phase mass transfer coefficient, m/s
k_m	membrane mass transfer coefficient, m/s
k_a^w	local air-phase mass transfer coefficient for water, m/s
k_m^w	local mass transfer coefficient due to membrane for water, m/s
K_L	overall liquid phase based mass transfer coefficient, m/s
K_G^w	overall gas phase based mass transfer coefficient for water, m/s
L	hollow fiber length, m
Q_a	air flow rate, m^3/s
Q_w	water flow rate, m^3/s
R	stripping factor Q_w/Q_aH
Re	Reynolds number ($d_o v^w/\nu$)
r	pore radius, m
r_c	module radius ($r_{in}<r_c<r_{out}$, in Fig. 2), m
r_{in}	outer radius of the center tube, m
r_{out}	inner radius of the membrane module, m
S	dimensionless Raoult's Law constant for water
Sc	Schmidt number (ν/D_w^{ch})
Sh	Sherwood number ($k_L d_o/D_w^{ch}$)
t	time, s
V	reservoir volume, m^3
v^a	air velocity outside the hollow fiber, m/s
v^w	aqueous solution velocity outside the hollow fiber, m/s
v'	average velocity within the module without hollow fibers, m/s
v^a	air velocity inside the hollow fiber, m/s
v^w	aqueous solution velocity inside the hollow fiber, m/s
X^w	water vapor concentration in the air phase, ppm
X_{sat}^w	saturated water vapor concentration, ppm
x	fraction of the pore filled with air
$1-x$	fraction of the pore filled with water

Greek letters

δ	pore length, m
ε	fiber porosity (dimensionless)
ν	kinematic viscosity of air/water, m^2/s
τ	pore tortuosity (dimensionless)

using the correlations of Lévéque [11], Knudsen and Katz [12] and Cussler [13], respectively:

$$\frac{1}{k_L} = 0.617\left(\frac{Ld_i}{v^w {D_w}^{ch^2}}\right)^{0.33} \quad (1)$$

$$\frac{1}{k_a H} = 45.5\frac{d_o^{0.4}\nu^{0.27}}{{v^a}^{0.6} D_c^{ch^{0.67}} H} \quad (2)$$

and

$$\frac{1}{k_m H} = \frac{\delta}{D_c^{ch} H} \quad (3)$$

It was noted that the predicted overall mass transfer coefficient was significantly higher than the observed

values [3]. This indicates that one or more of the individual mass transfer coefficient(s) predicted was/were higher than that observed and warrant further careful study.

Membrane resistance for polypropylene flat membranes was directly measured as a function of membrane thickness by Qi and Cussler [7] and Kreulen et al. [9] for systems with chemical reaction. The membrane pores were reported as being gas-filled. However, reported values differed by three orders of magnitude from each other [7,9]. Kreulen et al. [9] stated, without a plausible explanation, that the higher resistances observed by Qi and Cussler [7] were possibly due to wetting of pores. Malek et al. [14] stated that all the pores might not be totally dry and predicted that a number of pores at the inlet of the hollow fiber might become wetted across the full membrane thickness due to an operating pressure that was higher than the breakthrough pressure.

The objectives of this work were (1) to determine the magnitude of mass transfer resistance due to the membrane for the MAS process using pure water, as well as, chloroform as model VOC from aqueous solution; (2) to investigate the effect of air flow through the lumen side and liquid cross-flow on the shell side of a microporous polypropylene hollow fiber membrane module on mass transfer and air-side pressure drop; and (3) to study the applicability of MAS for removal/recovery of chloroform from aqueous solutions in the ppm range, which is more reflective of industrial wastewater as opposed to ppb levels investigated in previous MAS papers.

2. Theoretical

2.1. Mass transfer mechanism for pure water

Since no liquid phase resistance exists for the transport of water, resistances are only from the membrane and from the air phase. Then, the following equation is applicable:

$$\frac{1}{K_{\mathrm{L}}} = \frac{1}{K_{\mathrm{G}}^{\mathrm{w}} S} = \frac{1}{k_{\mathrm{m}}^{\mathrm{w}} S} + \frac{1}{k_{\mathrm{a}}^{\mathrm{w}} S} \tag{4}$$

The change in water vapor concentration in the air stream in the longitudinal direction on the lumen side of a single hollow fiber under steady-state conditions is given by (Fig. 1)

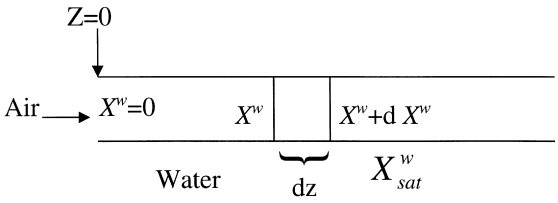

Fig. 1. Mass transfer in hollow fiber.

$$\frac{v^{\mathrm{a}}\,\mathrm{d}X^{\mathrm{w}}}{\mathrm{d}z} = K_{\mathrm{G}}^{\mathrm{w}} a (X_{\mathrm{sat}}^{\mathrm{w}} - X^{\mathrm{w}}) \tag{5}$$

Under the boundary conditions $X^{\mathrm{w}}=0$ at $z=0$ and $X^{\mathrm{w}} = X_{\mathrm{L}}^{\mathrm{w}}$ at $z=L$, the above equation leads to

$$X_{\mathrm{L}}^{\mathrm{w}} = X_{\mathrm{sat}}^{\mathrm{w}} (1 - \mathrm{e}^{-(K_{\mathrm{G}}^{\mathrm{w}} aL)/v^{\mathrm{a}}}) \tag{6}$$

$K_{\mathrm{G}}^{\mathrm{w}}$ can be calculated by Eq. (4), knowing $1/(k_{\mathrm{a}}^{\mathrm{w}} S)$ and $1/(k_{\mathrm{m}}^{\mathrm{w}} S)$. The air-phase mass transfer coefficient $k_{\mathrm{a}}^{\mathrm{w}} S$ can be estimated by Lévéque's correlation [11]:

$$\frac{1}{k_{\mathrm{a}}^{\mathrm{w}} S} = \frac{0.617}{S} \left(\frac{L d_{\mathrm{i}}}{v^{\mathrm{a}} D_{\mathrm{c}}{}^{\mathrm{w}2}} \right)^{0.33} \tag{7}$$

$1/(k_{\mathrm{m}}^{\mathrm{w}} S)$ can also be predicted using the following equation [6,9], which is similar to Eq. (3) but takes into account the membrane porosity and pore tortuosity:

$$\frac{1}{k_{\mathrm{m}}^{\mathrm{w}} S} = \frac{\delta \tau}{D_{\mathrm{eff}}^{\mathrm{w}} \varepsilon S} \tag{8}$$

For membranes having a mean pore size of less than 0.1 μm, the continuum as well as Knudsen diffusion should be taken into account [9]. The effective diffusion coefficient, D_{eff}, can be approximately estimated using the following relationship [15]:

$$D_{\mathrm{eff}} = \left(\frac{1}{D_{\mathrm{c}}} + \frac{1}{D_{\mathrm{Kn}}} \right)^{-1} \tag{9}$$

For dilute gases, the continuum diffusion coefficient, D_{c}, can be evaluated by an empirical equation developed by Fuller et al. [16] as well, the Knudsen diffusion coefficient, D_{Kn}, can be evaluated by an equation given by Evans et al. [17] and Cussler [13]. Control of continuum or Knudsen diffusion will depend on the values of reciprocal terms in Eq. (9).

The values of X_L^w predicted by Eq. (6) and X_L^w obtained experimentally will be referred to as predicted and experimental X_L^w, respectively, hereafter. If experimental and predicted X_L^w agree with each other, then the mass transport in membrane is simply diffusion through air-filled pores. If they do not, some other mechanisms, such as surface diffusion and capillary condensation, should be considered.

2.2. Mass transfer mechanism of chloroform

Mass transfer fundamentals for the transport of VOCs in an MAS system have been reviewed by Mahmud et al. [1]. According to this review, the change in organic concentration of the solution in a completely mixed reservoir of a batch MAS system with time can be described by the following linear relationship [3]:

$$\ln\left(\frac{C_0}{C_t}\right) = kt \tag{10}$$

A value for k is obtained, using Eq. (10), as the slope of the plot of $\ln(C_0/C_t)$ versus t. Substituting the value of k in the following equation, Eq. (11), will provide the overall liquid phase based mass transfer coefficient, K_L,for the system when air and liquid solution streams are on the lumen and the shell side, respectively [1]:

$$K_L = \frac{v^w}{aL}(1-R)^{-1}\ln\left\{\left[\frac{Q_w}{Q_w - Vk}\right](1-R)+R\right\} \tag{11}$$

The stripping factor, $R{=}Q_w/(Q_aH)$, which is the inverse of the conventional definition used in packed tower aeration (PTA) calculations (i.e. $R{=}(Q_aH)/Q_w$), is used here as a lumped parameter rather than a critical design parameter as in PTA.

Mass transfer of chloroform occurs across the membrane barrier from the liquid side to the air side and is swept away by the stripping air flow. Mass transfer in MAS involves three sequential steps [3,4]. Firstly, chloroform diffuses from the bulk aqueous solution across the liquid boundary layer to the membrane surface. Secondly, it diffuses through the air-filled pores and lastly, chloroform diffuses through the air boundary layer outside the membrane pore into the stripping air. As mass transfer resistances are considered to be proportional to the inverse of the corresponding mass transfer coefficients, the overall liquid phase based mass transfer resistance ($1/K_L$) can thus be expressed as follows:

$$\frac{1}{K_L} = \frac{1}{k_L} + \frac{1}{k_m H} + \frac{1}{k_a H} \tag{12}$$

The local liquid phase mass transfer coefficient, k_L, has been predicted based on the correlation developed by Kreith and Black [18] for heat transfer (Eq. (13)), and those developed by Yang and Cussler [4] (Eq. (14)) and Reed et al. [19] (Eq. (15)), for liquid cross-flow on the shell side of hollow fiber membrane modules:

$$\mathrm{Sh} = 0.39\mathrm{Re}^{0.59}\mathrm{Sc}^{0.33} \tag{13}$$

$$\mathrm{Sh} = 1.38\mathrm{Re}^{0.34}\mathrm{Sc}^{0.33} \tag{14}$$

$$\mathrm{Sh} = 1.4\left(\frac{d_o v^w}{D_w}\right)^{0.33} \tag{15}$$

$1/(k_aH)$ and $1/(k_mH)$ are given by correlations of Lévéque [11] and Qi and Cussler [6], respectively, similar to Eqs. (7) and (8), by replacing Raoult's Law constant by Henry's Law constant as follows:

$$\frac{1}{k_a H} = \frac{0.617}{H}\left(\frac{Ld_i}{v^a D_c{}^{ch2}}\right)^{0.33} \tag{16}$$

$$\frac{1}{k_m H} = \frac{\delta\tau}{D_{eff}^{ch}\varepsilon H} \tag{17}$$

2.3. Water velocity outside the hollow fibers

Water velocity outside the hollow fiber for the present study was evaluated using the following approach. As shown in Fig. 2, the module used in this study contains a central baffle that deflects the liquid flow on the shell side in the module and not the air flow on the lumen side of the fibers. The baffle blocks the center tube so that the incoming liquid exits the center tube in the upstream half of the tube, perpendicular to the fibers creating cross-flow. The liquid flows from the first compartment through the gap in between the middle baffle and the module housing to the second compartment. The liquid then flows across the fibers, enters the center tube and exits the module.

The water velocity in each compartment was first calculated assuming there were no hollow fibers in the

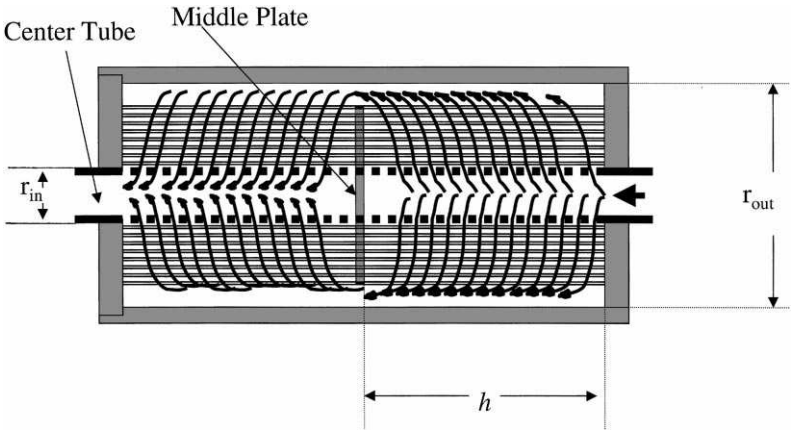

Fig. 2. The schematic view of cross-flow hollow fiber membrane module with liquid flow on the shell side.

module and then it was corrected using the void fraction. The length of each compartment, *h,* was half the module length, *L*, as the module was blocked in the center. It was assumed that the center tube was perforated such that water would flow through the entire cross-section of the center tube. Since the velocity of the liquid would decrease as it approached the module housing wall, a volume averaged velocity would be utilized in an empty module:

$$v' = \frac{\int (Q_w/(2\pi r_c h))dr_c}{\int dr_c} \tag{18}$$

$$v' = \frac{(Q_w/(2\pi h))\log\ r_c|_{r_{in}}^{r_{out}}}{r_c|_{r_{in}}^{r_{out}}} \tag{19}$$

$$v' = \frac{Q_w}{2\pi h}\frac{1}{r_{out}-r_{in}}\log\left(\frac{r_{out}}{r_{in}}\right) \tag{20}$$

Therefore, the final water velocity in between the hollow fibers in the module was

$$v^w = \frac{v'}{\text{void fraction}} \tag{21}$$

3. Experimental

3.1. Materials

Materials for this study were of analytical grade and were used without further purification, unless stated otherwise. The related values used for the compounds in this study are given in Table 1.

Chloroform with a purity of 99.8% (BDH Inc., Toronto, Ont., Canada) was used to prepare the feed solutions as well as the standards for gas chromatography analysis. Potassium hydrogen phthalate of

Table 1
Related values used for the compounds

Compound	Temperature (K)	Dimensionless partition coefficient	X_{sat}^{w} (ppm)	$D_c\times10^5$ (m^2/s)	$D_{Kn}\times10^4$ (m^2/s)	$D_w^{ch}\times10^9$ (m^2/s)
Water	294	0.0245[a]	15246[b]	2.50[c]	5.88[d]	
Chloroform	296	0.1475[e]		0.923[c]	2.29[d]	0.893[f]

[a] Raoult's Law constant for water calculated assuming 100% pure water.
[b] X_{sat}^{w}: saturated water concentration in air, calculated from saturated vapor pressure of water in air.
[c] D_c: continuum diffusion coefficient of the component in air phase, calculated (Fuller et al. [16] correlation).
[d] D_{Kn}: Knudsen diffusion coefficient, calculated [13,17].
[e] Henry's Law constant, calculated [20,21].
[f] D_w^{ch}: diffusion coefficient of chloroform in water, calculated [22], multiplied with a factor of 0.9 to match the observed deviation [13,23,24].

more than 99.9% purity (Kanto Chemical Co. Inc., Japan) was used as a standard for total carbon (TC)/ total organic carbon (TOC). Sodium hydrogen carbonate with a purity of more than 99.8% (Kanto Chemical Co. Inc., Japan) and anhydrous sodium carbonate with a purity of more than 99.7% (Kanto Chemical Co. Inc., Japan) were used as standards for inorganic carbon (IC). Orthophosphoric acid (Anachemia Science, Lachine, PQ, Canada) was used in the TC analysis. Water used throughout the study was reverse osmosis grade obtained from a Reverse Osmosis System (Model WMQ600, Zenon Environmental Inc., Burlington, Ont., Canada) with less than 50 ppb inorganic carbon.

3.2. Membrane module

A Liqui-Cel Extra-Flow 8 cm×28 cm (2.5 in.×8 in.) laboratory-scale membrane contactor with polypropylene microporous hollow fibers (Separation Products Division, Hoechst Celanese Corporation, Charlotte, NC, USA) was used. To consider the abnormality of pore shapes, a tortuosity factor of 2.5 has been used. Detailed specifications of the fiber and the module are given in Tables 2 and 3, respectively.

3.3. Experimental setup

A MAS experimental setup was designed to provide liquid cross-flow on the shell side and stripping air flow through the lumen side of the hollow fiber module (Fig. 3). The system included an aqueous solution/pure water feed circulation line and an air-stripping line. All connecting tubes were teflon tubes and were thermally insulated. The feed from a glass reservoir (volume=6.675×10^{-3} m^3) was circulated through the membrane module with a centrifugal micro pump. The temperature of the feed was maintained constant. The inline feed temperature was monitored before the membrane module inlet with a microcomputer thermometer (Model HH-72T, Omega Engineering, Mississauga, Ont., Canada). The pressure drop was measured using a precision digital pressure gauge (PG 5000, PSI-Tronix, Tulare, CA, USA).

The existence of a headspace in the reservoir during experiments with VOCs could lead to an error in the calculation of the overall mass transfer coefficient [1]. To eliminate headspace in the reservoir, the change in the liquid volume in the system due to sampling or mass transfer was compensated using a 10 ml hypodermic syringe (Becton Dickinson and Company, Franklin Lakes, NJ, USA) connected to the reservoir. About 1 ml of the solution was kept in the volume equalization syringe at all times to stop air from entering the reservoir. This approach easily and

Table 2
Hollow fiber membrane specifications

Characteristics	
Fiber outer diameter[a]	300 μm
Fiber inner diameter[a]	240 μm
Fiber wall thickness[a]	30 μm
Effective fiber length[b]	15 cm
Pore diameter[a]	0.03 μm
Pore tortuosity[c]	2.5
Porosity[a]	40%
Maximum transmembrane differential pressure[a]	414 kPa
Maximum operating temperature range[a]	1–60°C

[a] Supplied by manufacturer.
[b] Refer to [b] in Table 3.
[c] [25].

Table 3
Hollow fiber membrane module specifications

Characteristics	
Cartridge dimension[a]	8×28 cm (2.5 in.×8 in.)
Shell inside diameter[a]	5.55 cm
Center tube outer diameter[a]	2.22 cm
Shell side volume[a]	∼330 ml
Lumen side volume[a]	∼90 ml
Number of fibers[b]	9,950
Void fraction[c]	0.654
Effective membrane surface[a]	1.4 m^2
Effective surface to volume ratio[a], a	2930 m^2/m^3
Fiber potting material[a]	Polyethylene
Housing material[a]	Polypropylene
Housing maximum pressure[a]	414 kPa

[a] Supplied by the manufacturer.
[b] Manufacturer supplied information regarding effective fiber length and number of fibers as 0.16 m and 10 000, respectively. Schöner et al. [26] measured the effective fiber length and number of fibers as 0.15 m and 9950, respectively. Effective surface area provided by the manufacturer, matches to the calculated values using these numbers provided by Schöner et al. [26]. As the authors had no chance to open and measure them, they used the figures from Schöner et al. [26].
[c] Calculated.

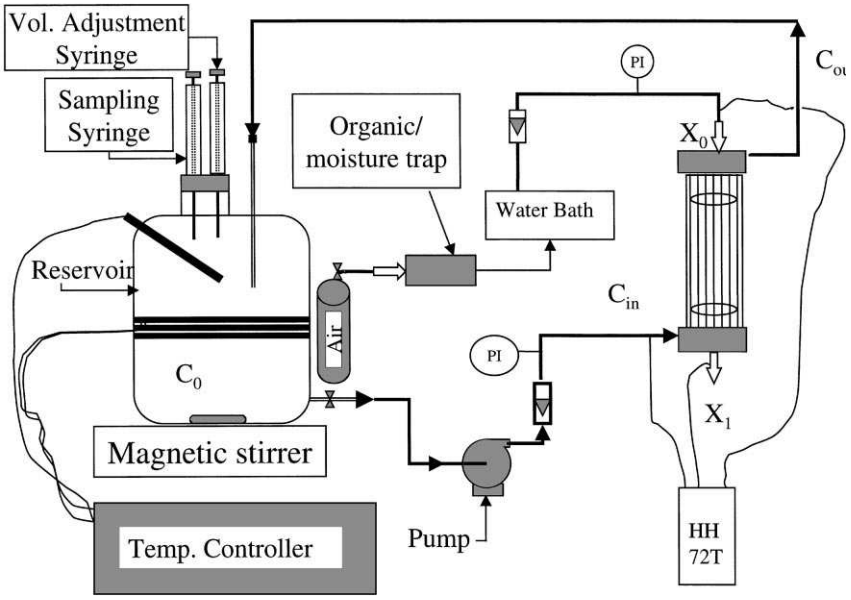

Fig. 3. Membrane air-stripping experimental setup.

inexpensively solved the potential headspace problem, eliminating the need for an expensive floating cover in a laboratory-scale setup.

Compressed air from an air cylinder (Praxair Products Inc., Mississauga, Ont., Canada) was passed through a hydrocarbon/moisture trap (Model HMT-200-4, Chromatographic Specialties Inc., Brockville, Ont., Canada) and a constant temperature water bath before it entered the membrane module. A precision digital pressure gauge (PG 5000, PSI-Tronix, Tulare, CA, USA) was used to monitor the pressure drop. The temperature of the air was maintained constant. In-line air temperatures were monitored before and after the module with a microcomputer thermometer (Model HH-72T, Omega Engineering, Mississuaga, Ont., Canada). The stripped air was released to a fume hood or passed through a cryo focus (cold trap) to trap the water moisture by condensation for analysis.

During the experiments, the feed solution was kept homogenous with a magnetic stirrer, and unless stated otherwise, by feed recirculation. A required volume of water was injected into the reservoir 30 s prior to each sample collection through the sampling port to compensate for the sample withdrawn for analysis as well as the reduction of liquid due to transport of water/VOC to the stripping air. After each test with chloroform solutions, the feed was drained from the system. Then, the system was filled with RO water and drained at least four times before the system was refilled with RO water. Water was circulated for 3–4 h with stripping air flow on the lumen side. Water was then drained and the system kept empty until the next test.

3.4. Analytical methods

Chloroform concentrations in the feed solutions were determined by measuring TC and TOC by a total carbon analyzer (Model TOC-5050, Shimadzu Corporation, Kyoto, Japan) and counter-checked by a gas chromatograph (Varian — Vista Series 6000, Varian Instrument Group, Walnut Creek Division, Walnut Creek, CA) to which a liquid purge and trap sample concentrator (Tekmar-LSC-2, Tekmar Company, Cincinnati, OH) was attached. The gas chromatographic system had a flame ionization detector (FID), operated with a packed column (Carbopack B 60/80 mesh, 1% SP-1000, 8 ft × 1/8 in. SS, Supelco Canada Ltd., Oakville, Ont.) and an integrator (Waters 820 Chromatography Data Station, Water Chromatography Division, Millipore Corporation, Milford, MA).

Gas tight syringes (Hamilton Co., Reno, NV) were used for sample collections.

3.5. Experiments for water transport

These experiments were conducted to determine the rate of water transport. Two types of experiments referred to as dry and wet tests were performed. In the dry tests, the shell side of the membrane module was dried by an air stream for over 72 h prior to the experiments. Then, the shell side of the module was filled with water, which was circulated for 30 min to get rid of any trapped air. The stripping air flow on the lumen side was started 10 min prior to the collection of the first sample to stabilize the system. The wet tests were prepared by filling the system with water and circulating for 48 h prior to starting the stripping air flow. This 48 h contact period was chosen based on the observation that wetting was stabilized after about 24–30 h of water contact and did not change after that during 70 h long tests. A period of 30 min of air flow was allowed to stabilize the system and to remove any condensed water in the fiber/module prior to sampling.

The total amount of water transported from the water phase (shell side) to the air phase (lumen side) was measured by trapping water vapor in the stripping air as it exited the module using a cryo focus immersed in liquid nitrogen. The transport rate was determined by weighing the amount of water condensed during a predetermined period. Stripping air flow rates were varied from 1.75×10^{-5} to 5.00×10^{-5} m^3/s and the liquid flow rate was maintained at 6.33×10^{-5} m^3/s. Pressure drops for air and water were about 0.5–2.0 and 20.0 kPa, respectively. Temperature was maintained at 21.0±0.2°C. The run times were between 10 and 61 min. A number of replicates were conducted at each air flow rate.

3.6. Experiments for the removal of chloroform from aqueous solutions

In these experiments, both dry and wet tests were conducted. For both groups of tests, concentrated chloroform feed solutions were prepared in a separate flask and the required volume was transferred to the reservoir. Trapped air, if any, was purged from the system. The feed solution was mixed by vigorous stirring in addition to feed circulation for 60 min prior to starting the stripping air flow. The first sample was collected 10 min after starting the stripping air flow to stabilize the system. In the preparation of the wet tests, the reservoir was filled with reverse osmosis grade water and circulated for 48 h. Before adding the chloroform solution, stripping air was passed on the lumen side for 30 min to remove any accumulated condensed water on the lumen of the fibers and stabilize the system. To add the concentrated chloroform solution, an equivalent quantity of water was drained while water circulation was continued through the module. For the dry tests, the reservoir was filled with reverse osmosis grade water just prior to addition of the concentrated chloroform solution. The samples were collected from the reservoir for analysis every 10 min in the beginning, but the interval was increased at the later stages. Stripping air flow rates were varied from 1.67×10^{-5} to 8.33×10^{-5} m^3/s, keeping the liquid flow rate constant at 3.33×10^{-5} m^3/s. Initial chloroform concentrations in the feed solutions were 680±30 ppm. The temperature of the solution as well as that of the air was kept at 23.0±0.2°C. Pressure drops for the air side and solution side were 0.2–3.0 and 10.0 kPa, respectively. The total run times for the dry and wet tests were 140 and 160 min, respectively.

3.7. Effect of feed chloroform concentration on overall mass transfer coefficient

A number of tests were conducted with initial feed chloroform concentrations in the range of 50–1000 ppm. These tests were carried out only under wet conditions in the same way as described in Section 3.6 except that the stripping air flow rate was kept constant at 5.83×10^{-5} m^3/s.

4. Results and discussion

4.1. Water transport

Fig. 4 shows X_L^w, the water concentration in the stripping air at the exit of the membrane module for different air flow rates. X_L^w was obtained from Eqs. (4) and (6) assuming the pores were filled with air throughout their entire length. The predicted X_L^w

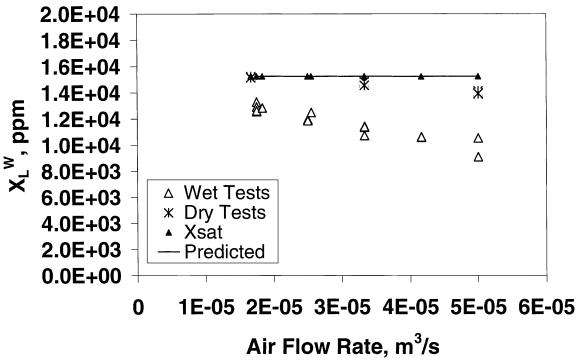

Fig. 4. X_L^w, water vapor concentration in stripping air at the exit.

was same as the saturated water vapor concentration in the air phase, X_{sat}^w (Fig. 4). It is clear from Fig. 4 that X_L^w's for the wet tests were lower than those for the dry tests when the remaining operating conditions were the same. It was also noticed that values of X_L^w for the dry tests were very close to X_{sat}^w. Thus, it can be concluded that the transport is dominated by diffusion through air-filled pores and the gas phase boundary outside the pores.

The experimental values of X_L^w for the wet tests were lower than those for the dry tests (Fig. 4). This indicates that the overall mass transfer resistances for the wet tests were higher than those for the dry tests. This led to the examination of what might have contributed to this additional mass transfer resistance. One possible reason for the presence of additional mass transfer resistance was that some pores were filled with water as claimed by Malek et al. [14]. In this study, it was unlikely as the pressure difference between the shell side and the lumen side was less than 20 kPa, while the required pressure for water to penetrate into the pores should be 4246 kPa according to the Young–Laplace equation [27,28].

Capillary condensation of water vapor in the pores or on the lumen side of the fiber was another possibility. But water vapor condensation on the lumen side of the fiber as observed by Côté et al. [29] was very unlikely since water transported to the lumen side was immediately swept away by stripping air stream. As mentioned in Section 3.5, air was passed through the lumen side for 30 min before collection of the first sample to remove any accumulated condensed water on the lumen side of the fibers. Moreover, some long-term experiments (up to 70 h) for MAS of water were conducted starting with a dry membrane with air flow on the lumen side as control. The decrease in water transport was similar to that without air flow on the lumen side. The observed pressure differences were the same for the wet and dry tests. Thus, it was extremely unlikely that certain fiber lumen be blocked by condensed water vapor. However, the air stream might not be able to remove the condensed water vapor in the pores. It appears that the form and location of condensed water and its impact on restricting the transport is not very clear. One possibility was that a layer of adsorbed water covered the pore walls that lead to reduction of the effective pore radius. Another was that droplets covered parts of the pores and narrowed the channel available for water diffusion. The pores in these membranes are known to be far from cylindrical. Capillary condensation could occur in the narrow radius portion of the irregularly-shaped pores. Thus, the mechanism of water transport through a partially wetted pore was not clearly understood. Further investigation in this regard was conducted with the MAS of chloroform from aqueous solution.

4.2. Removal of chloroform from aqueous solution

Experiments conducted for the MAS of chloroform from aqueous solutions under both dry and wet conditions confirmed the presence of additional mass transfer resistance for the wet tests compared to the dry tests. A typical example is presented in Fig. 5, which

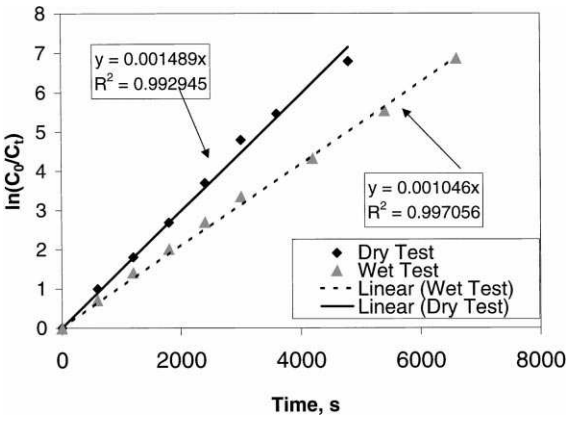

Fig. 5. Comparison between slopes for the dry and wet tests for MAS of chloroform.

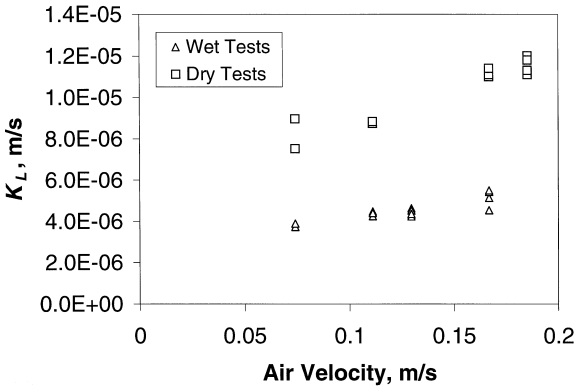

Fig. 6. Comparison of observed K_L for the dry and wet tests for chloroform at liquid flow rate of 3.33×10^{-5} m^3/s.

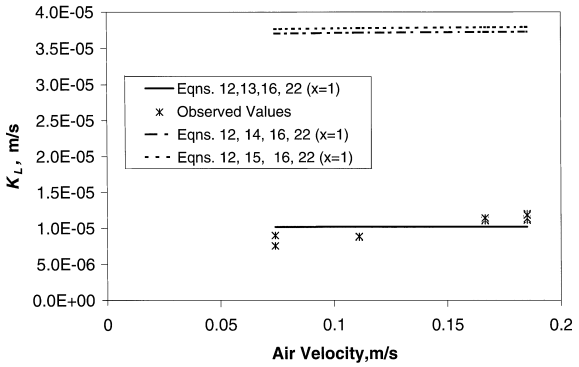

Fig. 7. Comparison between predicted and observed K_L for MAS of chloroform (dry test).

shows a significantly higher slope (faster removal of chloroform) for the dry tests than for the wet tests, while the other operating conditions were identical. The observed overall mass transfer coefficient, K_L, was calculated from the slope using Eq. (11) for both dry and wet tests and is compared in Fig. 6.

Considering capillary condensation of water vapor in the pores, an assumption was made that water penetrated into and filled a portion of the pore, and chloroform molecules were transported through this water layer by diffusion. Then, the mass transfer resistance due to membrane was predicted using the following modified equation:

$$\frac{1}{k_m H} = x\frac{\delta\tau}{D_{eff}^{ch}\varepsilon H} + (1-x)\frac{\delta\tau}{D_w^{ch}\varepsilon} \tag{22}$$

Fig. 7 presents K_L values for the dry tests generated experimentally and those predicted by three models using x=1.0. These model predictions combined Eqs. (12), (16) and (22) and different equations for the local liquid-phase mass transfer coefficient. These were Eqs. (13)–(15) developed by Kreith and Black [18], Yang and Cussler [4] and Reed et al. [19], respectively. The Kreith and Black [18] correlation yielded better predictions than the correlations of Yang and Cussler [4] and Reed et al. [19]. A similar analysis was carried out for the wet tests after adjusting the value of x=0.6 to fit the data (Fig. 8) and the Kreith and Black [18] correlation was again found to be superior. It should be noted that Yang and Cussler [4] expected the Kreith and Black [18] correlation, developed for cross-flow in closely packed tube bank, would describe their data but it did not. However, geometrically, the two systems were very similar. One of the reasons might be as reported by Yang and Cussler [4] that the module was prepared in the laboratory and the fibers were sufficiently separated to behave as single cylinders rather than being a closely packed bundle of fibers. The fibers in the module used in the present study were closely packed and had liquid cross-flow and might be comparable to the system used by Krieth and Black [18], thereby predicting our data better.

The values of $1/k_L$, $1/(k_a H)$ and $1/(k_m H)$ were calculated using Eqs. (13), (16) and (22) using x=1.0 for the dry tests and x=0.6 for the wet tests, respectively, for air and liquid flow rates of 3.33×10^{-5} m^3/s. The overall mass transfer resistance $1/K_L$ was obtained adding individual resistances as per Eq. (12).

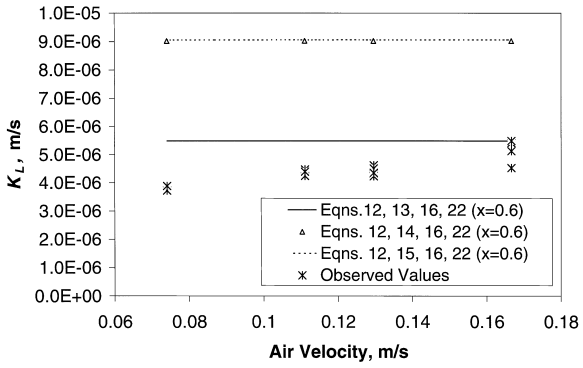

Fig. 8. Comparison between predicted and observed K_L for MAS of chloroform (wet test).

The value of $1/(k_m H)$ calculated for the wet tests in this study was two orders of magnitude higher than that for the dry tests and was almost equal to the liquid-phase resistance. Thus, its contribution to the overall mass transfer resistance became significant. In commercial applications, the operating period of MAS is usually long, hence it is more natural to consider that the pores are partially wetted. This aspect has to be taken into account in the design of MAS units. The value of $1/(k_m H)$ for the dry tests was calculated by Eq. (22) to be 142.77 s/m by setting x=1.0, thus $1/k_m$ was 21.13 s/m after taking Henry's Law constant into account. This value is comparable to 33.33 s/m reported by Kreulen et al. [9] as $1/k_m$. On the other hand, $1/(k_m H)$ for the wet tests was calculated to be 8.41×10^4 s/m by setting x=0.6. This value is also comparable to the value of 10^5 s/m, measured by Qi and Cussler [7], who presumed it was so for air-filled pores. The comparison of partially wet and dry pores in this work explains Kreulen et al.'s [9] conjecture that the pores in Qi and Cussler's work [7] were partially wetted. Despite the differences in the systems studied by Kreulen et al. [9], Qi and Cussler [7] and the present authors, the resulting membrane mass transfer resistances are comparable.

Applying Eqs. (1), (2), (12) and (22) at x=0.65, the overall mass transfer coefficients of chloroform were predicted and the results were compared with the data of Semmens et al. [3]. Only continuum diffusion was considered in our calculations to keep consistency with the original paper. The agreement between predicted and observed values is very good as shown in Fig. 9. The slight differences in values of x between Semmens et al. [3] and the present study are likely dependent on the experimental conditions. The lack of consideration for the wet/dry state of the pores may also explain different overall mass transfer resistances obtained by other researchers.

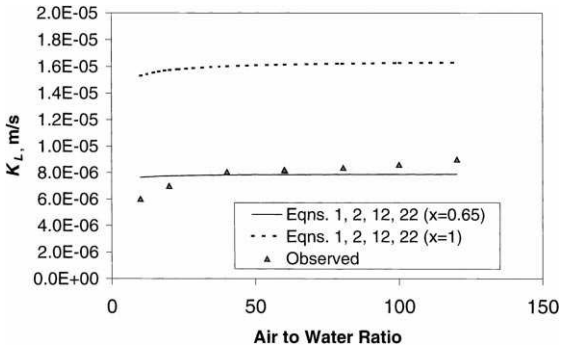

Fig. 9. Comparison between predicted K_L with or without liquid in the pores and observed K_L by Semmens et al. [3].

The overall mass transfer coefficients obtained in this work for the removal of chloroform from aqueous solution were double of those reported by Semmens et al. [3], whose batch system had the same air velocities on the shell side and at least an order of magnitude higher water velocities on the lumen side. The K_L values from the present study were comparable to those reported by Zander et al. [8] who used a continuous flow (single pass) system and had air velocities on the shell side at least three times higher and an order of magnitude higher water velocities on the lumen side than this study. A higher overall mass transfer coefficient of oxygen was also obtained by Sengupta et al. [30] for modules with liquid cross-flow on the shell side as compared with liquid flow on the lumen side.

In this study, liquid velocity was kept constant, thus the liquid film resistance should be constant. The mass transfer resistance due to the membrane should not change with the change of air or liquid velocity. The overall mass transfer coefficients of chloroform increased with an increase in air velocity for both wet and dry tests (Figs. 6 and 7), as expected by the reduction of the gas film resistance. However, the sensitivity to the variation in air velocity was much stronger than predicted. Further detailed study is required to understand this phenomenon, better.

4.3. Effect of feed chloroform concentration

Fig. 10 shows the effect of chloroform feed concentration on overall mass transfer coefficient. From the figure, it is clear that there is no effect of initial feed chloroform concentration in the range of 50–1000 ppm studied, so this technology has potential for industrial wastewater applications.

4.4. Air pressure drop on the lumen side of hollow fiber

The pressure drop caused by air flow on the lumen side was studied both experimentally and theoretically. The theoretical calculation was done by the Hagen–Poiseuille equation. The experimental values

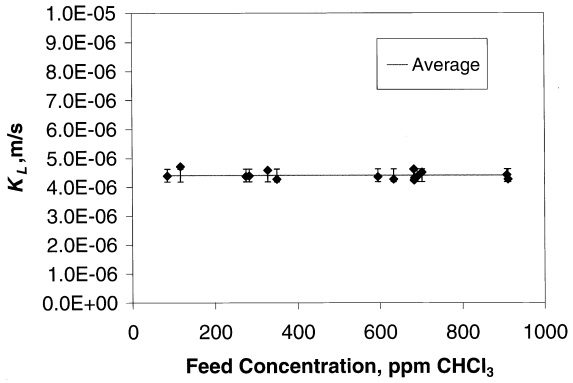

Fig. 10. Effect of feed $CHCl_3$ concentration on K_L.

were an order of magnitude higher than theoretical ones. Data provided by the manufacturer for air pressure drop on the lumen side [31] were four times higher than those predicted by Hagen–Poiseuille. It needs to be pointed out that this observed pressure drop was a combined effect of the pressure drop caused by the air flow on the lumen side as well as at the inlet and outlet of the module. The experimental values in this study were about five times higher than those reported for the shell side by Zander et al. [8]. A higher pressure drop by a factor of four on the lumen side compared to that on the shell side for liquid flow was also reported by Sengupta et al. [30].

5. Conclusions

The polypropylene hollow fiber membrane pores were almost completely air-filled for a short period of time after coming in contact with an aqueous phase. During this condition, the mass transport through these pores was simply diffusion through air and its contribution to the overall mass transfer resistance was negligible.

The pores appeared to become partially wetted or blocked by water due to their prolonged contact with water during air-stripping operation. The deposition of water in the pores created a liquid barrier and led to a higher membrane resistance. In this situation, diffusion through air as well as liquid in the pores needed to be taken into account.

A model that considers the membrane resistance to be composed of (1) a resistance for the fraction of pores that are air-filled, (2) a resistance for the fraction of pores that are liquid-filled has been proposed. The model predictions agree very well with our experimental data as well as that from the literature.

The mass transfer resistance created by the membrane when partially wetted was almost equal to liquid phase resistance and its contribution to the overall mass transfer resistance became significant.

The Kreith and Black [18] correlation provides better predictions in these closely packed membrane modules having liquid cross-flow on the shell side compared to the correlations of Yang and Cussler [4] and Reed et al. [19].

No effect of feed chloroform concentration was observed on the overall mass transfer coefficient within the range of concentration (50–1000 ppm) studied in this work. Thus, MAS has a great potential for removal/recovery of VOCs from VOCs laden industrial wastewater.

Although, liquid cross-flow on the shell side yielded a higher overall mass transfer coefficient than that on the lumen side, the air pressure drop on the lumen side was significantly higher than that of shell side.

References

[1] H. Mahmud, A. Kumar, R.M. Narbaitz, T. Matsuura, Hollow fiber membrane air stripping: a process for removal of organics from aqueous solutions, Sep. Sci. Technol. 33 (14) (1998) 2241–2255.

[2] A. Kiani, R.R. Bhave, K.K. Sirkar, Solvent extraction with immobilized interfaces in a microporous membrane, J. Membr. Sci. 20 (1984) 125–145.

[3] M.J. Semmens, R. Qin, A. Zander, Using a microporous hollow-fiber membrane to separate vocs from water, J. Am. Water Works Assoc. 81 (4) (1989) 162–167.

[4] M.C. Yang, E.L. Cussler, Designing hollow-fiber contactors, AIChE J. 32 (11) (1986) 1910–1916.

[5] Z. Qi, E.L. Cussler, Microporous hollow fibers for gas absorption. I. Mass transfer in the liquid, J. Membr. Sci. 23 (1985) 321–332.

[6] Z. Qi, E.L. Cussler, Microporous hollow fibers for gas absorption. II. Mass transfer across the membrane, J. Membr. Sci. 23 (1985) 333–345.

[7] Z. Qi, E.L. Cussler, Hollow fibers gas membranes, AIChE J. 31 (9) (1985) 1548–1553.

[8] A.K. Zander, M.J. Semmens, R.M. Narbaitz, Removing VOCs by membrane stripping, J. Am. Water Works Assoc. 81 (11) (1989) 76–81.

[9] H. Kreulen, C.A. Smolders, G.F. Versteeg, W.P.M. Van Swaaij, Determination of mass transfer rates in wetted and

non-wetted microporous membranes, Chem. Eng. Sci. 48 (11) (1993) 2093–2102.
[10] M. Bhowmick, M.J. Semmens, Batch studies on a closed loop air stripping process, Water Res. 28 (9) (1994) 2011–2019.
[11] J.A. Lévéque, Les Lois de la transmission de chaleur par convection, Annales de Mines 13 (1928) 201–299.
[12] J.G. Knudsen, D.L. Katz, Fluid Dynamics and Heat Transfer, McGraw-Hill, New York, 1958.
[13] E.L. Cussler, Diffusion. Mass Transfer in Fluid Systems, Cambridge University Press, London, 1984.
[14] A. Malek, K. Li, W.K. Teo, Modeling of microporous hollow fiber membrane modules operated under partially wetted conditions, Ind. Eng. Chem. Res. 36 (1997) 784–793.
[15] W.G. Pollard, R.D. Present, On gaseous self-diffusion in long capillary tubes, Phys. Rev. 73 (7) (1948) 762–774.
[16] E.N. Fuller, P.D. Schettler, J.C. Giddings, A new method for prediction of binary gas-phase diffusion coefficients, Ind. Eng. Chem. 58 (2) (1966) 19–27.
[17] R.B. Evans, G.M. Watson, E.A. Mason, Gaseous diffusion in porous media at uniform pressure, J. Chem. Phys. 35 (6) (1961) 2076–2083.
[18] F. Kreith, W.Z. Black, Basic Heat Transfer, Harper & Row, New York, 1980.
[19] B.W. Reed, M.J. Semmens, E.L. Cussler, Membrane contactors, in: R.D. Noble, S.A. Stern (Eds.), Membrane Separations Technology, Principles and Applications, Elsevier, New York, 1995, pp. 143–211.
[20] J.M. Montgomery, Water Treatment Principles and Design, Wiley, New York, 1985, pp. 239–240.
[21] D.A. Cornwell, Air stripping and aeration, in: F.W. Pontius (Ed.), Water Quality and Treatment, A Handbook of Community Water Supplies, 4th Edition, American Water Works Assoc., McGraw-Hill, New York, 1990, pp. 229–268.
[22] C.R. Wilke, P. Chang, Correlation of diffusion coefficients in dilute solutions, AIChE J. 1 (2) (1955) 264–270.
[23] J.H. Smith, D.C. Bomberger, D.L. Haynes, Prediction of the volatilization rates of high-volatility chemicals from natural water bodies, Environ. Sci. Technol. 14 (11) (1980) 1332–1337.
[24] P.V. Roberts, P.G. Dändiliker, Mass transfer of volatile organic contaminants from aqueous solution to the atmosphere during surface aeration, Environ. Sci. Technol. 17 (8) (1983) 484–489.
[25] R. Prasad, K.K. Sirkar, Dispersion-free solvent extraction with microporous hollow-fiber modules, AIChE J. 34 (2) (1988) 177–187.
[26] P. Schöner, P. Plucinski, W. Nitsch, U. Daiminger, Mass transfer in the shell side of cross-flow hollow fiber modules, Chem. Eng. Sci. 53 (13) (1998) 2319–2326.
[27] J.T.F. Keurentjes, J.G. Harbrecht, D. Brinkman, J.H. Hanemaaijer, M.A. Cohenstuart, K. Van't Riet, Hydrophobicity measurements of microfiltration and ultrafiltration membranes, J. Membr. Sci. 47 (1989) 333–344.
[28] N.P. Tirmizi, B. Raghuraman, J. Wiencek, Demulsification of water/oil/solid emulsions by hollow-fiber membranes, AIChE J. 42 (5) (1996) 1263–1275.
[29] P. Côté, J.L. Bersillon, A. Huyard, Bubble-free aeration using membranes: mass transfer analysis, J. Membr. Sci. 47 (1989) 91–106.
[30] A. Sengupta, P.A. Peterson, B.D. Miller, J. Schneider, C.W. Fulk Jr., Large-scale application of membrane contactors for gas transfer from or to ultrapure water, Sep. Purif. Technol. 14 (1998) 189–200.
[31] J.T. Whisnant, Sales Representative, Hoechst Celanese, Personal Communication, 1999.